AIAA JOURNAL
Vol. 44, No. 1, January 2006

Analysis Tools for Adhesively Bonded Composite Joints, Part 1: Higher-Order Theory

Brett A. Bednarcyk*
University of Virginia, Charlottesville, Virginia 22903
James Zhang† and Craig S. Collier‡
Collier Research Corporation, Hampton, Virginia 23669
and
Yogesh Bansal§ and Marek-Jerzy Pindera¶
University of Virginia, Charlottesville, Virginia 22903

A new application of the higher-order theory to the analysis of adhesively bonded composite joints is investigated. The adhesively bonded joint problem is currently of interest to the aerospace field because of the heavy reliance on bonded composite structures in an extensive number of new aircraft designs. As such, new tools that enable the sizing of joints in the context of the overall vehicle design are being sought. Through comparison of analytical and finite element results from the literature, along with a recently developed unified analytical joint analysis methodology, it is shown that the higher-order theory is a capable tool for joint analysis that serves as a middle ground between the finite element approach and less general analytical methodologies. In Part 2 of the paper, an alternative analytical method for the three-dimensional stress analysis of composite bonded joints will be investigated.

I. Introduction

THE analysis of adhesively bonded joints continues to be a relevant problem as tools are sought to enable design of advanced structures fabricated using bonded components. The bonded joint problem is particularly pertinent to the aerospace field as the next generation of aircraft, such as the joint strike fighter, the long-range strike aircraft, and new unmanned aerial vehicles, will rely heavily on adhesively bonded polymer matrix composite structures. Although tools and procedures have been developed for rapid design, analysis, and sizing of aerospace structures from the level of the vehicle to the level of the stiffened panel component (HyperSizer®),[1] a weak link in the design process remains the automated sizing of joints between structural components. This motivates the investigation of new joint analysis techniques like the higher-order theory.

The adhesively bonded joint problem is typically approached in one of two ways: with finite element analysis (FEA) or through analytical modeling. FEA has the advantage of geometric flexibility and the availability of commercial FEA codes. Examples of FEA investigations of adhesively bonded composite joints include Kairouz and Matthews,[2] Shenoi and Hawkins,[3] Tsai et al.,[4] Yamazaki and Tsubosaka,[5] Tong,[6] Li et al.,[7] Krueger et al.,[8,9] and Bogdanovich and Kizhakkethara.[10] The literature shows that standard h-based FEA codes can do a good job of predicting the local stress fields within adhesively bonded joints under arbitrary loading conditions. However, this approach can suffer in terms of efficiency, and its high level of mesh dependence limits its applicability to design and sizing, where a large number of different joint configurations might need to be considered and analyzed. P-based FEA codes such as StressCheck** improve local field predictions by altering the order of the elements' polynomials rather than requiring successively finer element meshes to capture concentrations. As such, the Composites Affordability Initiative has selected StressCheck as a potential design tool for adhesively bonded joints.

The analytical approach to adhesively bonded joint analysis typically employs simplifying assumptions in terms of the joint geometry, loading, and resultant local fields in order to formulate an efficient, closed-form, elasticity solution for the local fields in the joint region. The analytical approach has its roots in classical shear-lag analysis of Volkersen[11] and the work of Goland and Reissner,[12] who accounted for bending in the analysis of a bonded single lap joint. Hart-Smith[13–18] extended these solutions to account for the inelastic behavior of the adhesive and considered many joint and adherend configurations. However, the Hart-Smith formulations are limited in terms of the applied loading considered and the one-dimensional treatment of the adherends with an effective stiffness in the joint direction. More recently, Mortensen[19] and Mortensen and Thomsen[20,21] presented a unified analytical approach to solve for the local fields in an array of common bonded joint configurations for more general loading conditions. Mortensen's treatment also considers arbitrary laminate adherends [based on their extensional, coupling, and bending stiffness (ABD) matrices] and solves for the distributions of the normal and shear force and moment resultants along the joint in all adherends (as well as peel and shear-stress distributions in the adhesive). Further, through the application of an efficient solution algorithm, convergence issues that arise in Hart-Smith's formulations have been overcome.

The main objective of the current paper is to present and determine the utility of a new approach to the adhesively bonded joint problem based on the higher-order theory for functionally graded materials (HOTFGM).[22] As the name implies, this theory was originally developed for the analysis of functionally graded materials,[23–26] but it has since been extended to admit structures with arbitrary cross sections.[27] Recently, the theory has been reformulated by Bansal and Pindera,[28] thereby simplifying the development of the original theory, which takes a circuitous approach and involves complex algebraic manipulations. This reformulation, which uses a local-global approach, makes possible the analysis of more refined and realistic

Presented as Paper 2004-1563 at the AIAA/ASME/ASCE/AHS/ASC 45th Structures, Structural Dynamics, and Materials Conference, Palm Springs, CA, 19–22 April 2004; received 12 July 2004; revision received 30 March 2005; accepted for publication 2 April 2005.

*Visiting Senior Research Scientist, Department of Civil Engineering. Member AIAA.
†Research Engineer, 2 Eaton Street, Suite 504. Member AIAA.
‡Research Engineer, 2 Eaton Street, Suite 504. Senior Member AIAA.
§Research Assistant, Applied Mechanics, Thornton Hall B228, 351 McCormick Road.
¶Professor, Department of Civil Engineering.

**Data available online at http://www.esrd.com [cited 14 May 2003].

microstructures that are computationally prohibitive in the original theory. Like the finite element method, HOTFGM considers a discretized geometry, but exhibits considerably less mesh dependence as continuity and field equations (heat transfer and equilibrium) are satisfied in a surface- and volume-averaged sense, respectively. As such, the HOTFGM formulation does not rely on nodes or a variational principle and is, in fact, a semi-analytical elasticity-based methodology. Further, because of the inherent Cartesian geometry employed by HOTFGM, the method is well suited for many joint geometries, whose cross sections can be represented by a number of rectangular subvolumes. The semi-closed-form nature of the theory renders it well suited for rapid design and sizing, while the availability of local fields, that can be used to predict local failure, allows HOTFGM to function ably within the HyperSizer[1] toolset.

The present investigation employs HOTFGM to analyze adhesively bonded composite double lap and bonded doubler joints. Results are compared to the recently developed solutions of Mortensen[19] for the double lap joint and the closed-form solution of Delale et al.[29] for the bonded doubler joint. In addition, the HOTFGM and Mortensen[19] double lap joint results are compared to Tong's[6] h-based FEA results and StressCheck** p-based FEA results, both of which considered inelastic adhesive behavior and included failure load predictions. Finally, HOTFGM is employed to analyze a more complex joint geometry (a so-called "tee joint") for which analytical models are lacking, and results are compared to the FEA results of Apalak et al.[30] The results of this paper indicate that HOTFGM is useful and quite accurate for the analysis of adhesively bonded joints. The approach appears to embody a middle ground spanning the accurate and versatile yet cumbersome finite element approach and the efficient yet somewhat limited analytical approach.

II. Model Description

The HOTFGM method was originally developed for functionally graded materials; however, it is equally applicable to any homogeneous or heterogeneous medium. For a full derivation of the HOTFGM theory, see Aboudi et al.[22] The geometry considered by HOTFGM is shown in Fig. 1. In this version of the model, the medium is finite in the x_2-x_3 plane and infinite in the x_1 direction. The medium is discretized into an arbitrary number of cells, each of which contains four subcells. Note that, although the present work employed the original HOTFGM formulation in which subcells are retained, it has recently been determined that the concept of subdivision of generic cells into subcells is redundant and can be discarded.[28] Each subcell can contain a distinct material, giving rise to a heterogeneous configuration. Loading takes the form of time-dependent thermal and mechanical boundary conditions, which are imposed at the free surfaces. The present work involves isothermal loading, and thus emphasis is placed on the HOTFGM solution for the mechanical problem. The displacement field in the subcell $(\beta\gamma)$ of the (q, r)th generic cell is approximated by a second-order expansion in the local coordinates $\bar{x}_2^{(\beta)}$ and $\bar{x}_3^{(\gamma)}$ as follows:

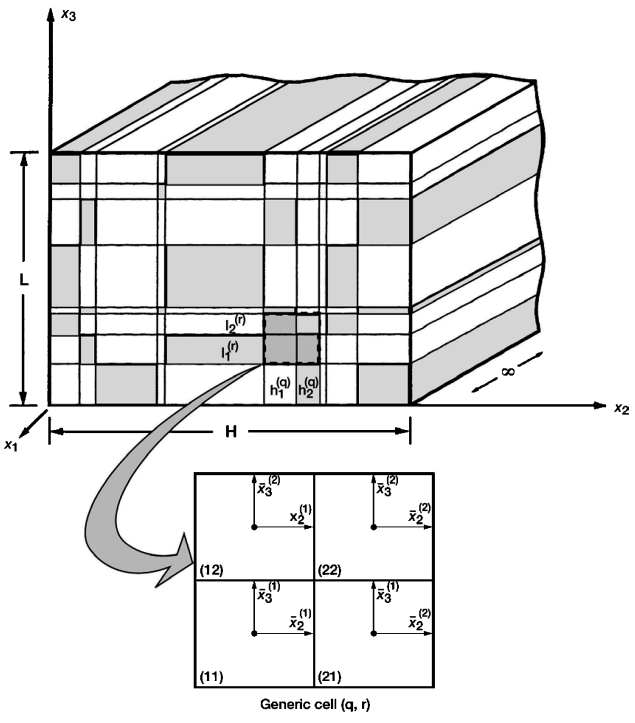

Fig. 1 HOTFGM analysis geometry.

$$u_2^{(\beta\gamma)} = W_{2(00)}^{(\beta\gamma)} + \bar{x}_2^{(\beta)} W_{2(10)}^{(\beta\gamma)} + \bar{x}_3^{(\gamma)} W_{2(01)}^{(\beta\gamma)} + \tfrac{1}{2}\left[3\bar{x}_2^{(\beta)^2} + \tfrac{1}{4}h_\beta^{(q)^2}\right] W_{2(20)}^{(\beta\gamma)} + \tfrac{1}{2}\left[3\bar{x}_3^{(\gamma)^2} + \tfrac{1}{4}l_\gamma^{(r)^2}\right] W_{2(02)}^{(\beta\gamma)} \quad (1)$$

$$u_3^{(\beta\gamma)} = W_{3(00)}^{(\beta\gamma)} + \bar{x}_2^{(\beta)} W_{3(10)}^{(\beta\gamma)} + \bar{x}_3^{(\gamma)} W_{3(01)}^{(\beta\gamma)} + \tfrac{1}{2}\left[3\bar{x}_2^{(\beta)^2} + \tfrac{1}{4}h_\beta^{(q)^2}\right] W_{3(20)}^{(\beta\gamma)} + \tfrac{1}{2}\left[3\bar{x}_3^{(\gamma)^2} + \tfrac{1}{4}l_\gamma^{(r)^2}\right] W_{3(02)}^{(\beta\gamma)} \quad (2)$$

where the 40 coefficients $W_{i(00)}^{(\beta\gamma)}$ (which are the displacements at the center of the subcell) and $W_{i(mn)}^{(\beta\gamma)}$ $(i = 2, 3)$ (the higher-order terms) serve as the unknown quantities. A system of equations is developed through the imposition of traction and displacement continuity in an average sense at the various interfaces within the medium. For boundary cells, the continuity of displacements and tractions is replaced by the applied mechanical boundary conditions. In addition, the equations of equilibrium are satisfied in a volume-averaged sense, and the resulting system of $40\,N_q\,N_r$ algebraic equations is symbolically represented by

$$\boldsymbol{KU} = \boldsymbol{f} + \boldsymbol{g} \quad (3)$$

where the structural stiffness matrix $\boldsymbol{K}$ contains information on the geometry and thermomechanical properties of the individual subcells $(\beta\gamma)$ within the cells comprising the medium, the displacement coefficient vector $\boldsymbol{U}$ contains the unknown coefficients that describe the displacement field in each subcell, the mechanical force vector $\boldsymbol{f}$ contains information on the imposed boundary conditions, and the inelastic force vector $\boldsymbol{g}$ contains information on the inelastic effects. Note that N_q and N_r are the total number of cells contained within the medium in the x_2 and x_3 directions, respectively.

The HOTFGM formulation allows the inelastic behavior of any constituent material to be simulated by an arbitrary viscoplastic model. Herein, the adhesive layer within the joint will be modeled (in some cases) using incremental plasticity theory.[31] In the presence of inelasticity, the loading on the medium must be applied incrementally, and a solution must be determined at each increment of the applied loading. In addition, for nonisothermal loading and temperature-dependent material properties, the system of Eqs. (3) must be solved at each increment of the applied loading. It is thus important to take advantage of the sparse nature of the matrix $\boldsymbol{K}$ to maximize the computational efficiency of the model.

Although HOTFGM is like FEA in that it considers a discretized geometry upon which boundary conditions are imposed, the formulation is completely unrelated to the finite element approach. HOTFGM is not explicitly formulated based on a variational principal, nor does it employ nodes. The governing equations are enforced in a volume-averaged sense for each subcell, as are the continuity conditions. As in the finite element method, refinement of geometric discretization does lead to improved field accuracy within HOTFGM, although the effect is less pronounced.

III. Results and Discussion

A. Bonded Doubler Joint

Delale et al.[29] developed a method for analysis of single lap joints and bonded doubler joints (stiffened plates) under normal, shear, and bending loads by considering the transverse shear in isotropic/orthotropic adherends and the in-plane normal strains in the adhesive. In this method, the adherends were treated as plates,

and the adhesive layer was treated as a tension-shear spring by neglecting the thickness. Different from conventional spring models, the method also takes into account the effect of the average longitudinal in-plane strain. The bonded joint problem can then be solved in closed form with the resulting adhesive stresses exhibiting good agreement with those obtained by the finite element method.[29]

The bonded doubler joint under uniaxial tension, studied by Delale et al.,[29] has been employed as a validation case for comparison to HOTFGM. The joint configuration, which is shown in Fig. 2, is identical to that analyzed by Delale et al.[29] The joint consists of an aluminum plate with a boron/epoxy laminate doubler. The homogenous material properties of the joint materials are given in Table 1.

Linear elastic analyses were performed for the bonded doubler joint using HOTFGM. The results were then compared with results of the closed-form solution of Delale et al.[29] Figure 3 shows the HOTFGM subcell discretization for the solution domain of the bonded doubler joint. Note that subcell discretization sensitivity studies were performed before arriving at this final subcell representation. Because of symmetry about the zy plane (Fig. 2), only half of the structure is used for analysis by applying symmetric boundary conditions at $x = 0$. The doubler has been discretized into 80 subcells in the x direction and 32 subcells in the z direction. A total of 48×8 subcells are used in the adhesive region. In the Delale et al.[29] model, a unit normal-force resultant was applied at the right end of the plate (Fig. 2), and correspondingly, a uniform traction of (1 N/mm)/(2.29 mm) (height of Al plate) = 0.4367 MPa was applied to the right end of the plate in HOTFGM (Fig. 3). Note that the adhesive stresses do not vary through the thickness in the model of Delale et al.[29] because of the spring model used. As such, in the case of the HOTFGM solution (in which adhesive stresses do vary through the thickness), the adhesive stress results are plotted at the central elevation of the adhesive.

Table 1 Elastic properties of the materials in the bonded doubler joint[29] (see Fig. 2)

Material	E_x, GPa	E_y, GPa	G_{zx}, GPa	ν_{zx}
Boron/epoxy	223.4	24.13	8.48	0.23
Aluminum	68.95	68.95	26.5	0.30
Epoxy adhesive	3.07	3.07	1.138	0.35

Figures 4a and 4b show the predicted adhesive shear and peel stresses based on these two analyses. As is well known, the stress concentrations at the bimaterial interface corners tend to be a power singularity when the adherend and adhesive are considered as elastic continua. However, the peak values of shear and peel stress in the adhesive are found to be finite peaks at the end of points $x = \pm$L in the solution of Delale et al.[29] This is because of the inherent limitation of the spring-type model employed for the adhesive in the analysis. The results given by HOTFGM also show a finite peak value of peel stress at the free edge. Because it is a traction at the free edge, the HOTFGM prediction for the adhesive shear stress τ_{xz} returns to zero at this location. With the exception of the near-free-edge shear-stress profile, the adhesive stresses predicted by HOTFGM are in excellent qualitative agreement with the predictions of Delale et al.[29] Quantitatively, the predicted peak values exhibit reasonable agreement between the two methods, even though some discrepancy exists. Specifically, for the current joint system, the solution of Delale et al.[29] predicts somewhat higher magnitude values of the peak peel and shear stresses compared to the predictions of HOTFGM.

B. Double Lap Joint

The second adhesively bonded joint configuration modeled using HOTFGM is the double lap joint (Fig. 5). Comparison is made to h-based FEA results of Tong,[6] as well as results of Mortensen's[19] semi-analytical method and of the p-based finite element code StressCheck.** Experimental joint failure data reported by Tong[6] are also used for comparison. It is worthy of mentioning that the unified solutions of Mortensen[19] can be applied to various joint configurations such as single lap, double lap, stepped, and scarfed joints with either straight or scarfed adherends, and with arbitrary loading and boundary conditions. Mortensen's[19] formulation assumes that the adherends undergo cylindrical bending, while the adhesive is treated as a linear or nonlinear spring. In addition, Mortensen's[19] model considers general situations for the adherend materials, such as when the adherends are asymmetric and unbalanced composite laminates. Recent publications[20,21] and parametric studies performed by the present authors have shown that Mortensen's[19] unified approach is robust, efficient, and accurate, and thus represents a promising analysis tool for adhesively bonded joints.

The StressCheck results reported herein have been obtained directly from Engineering Software Research and Development, Inc.

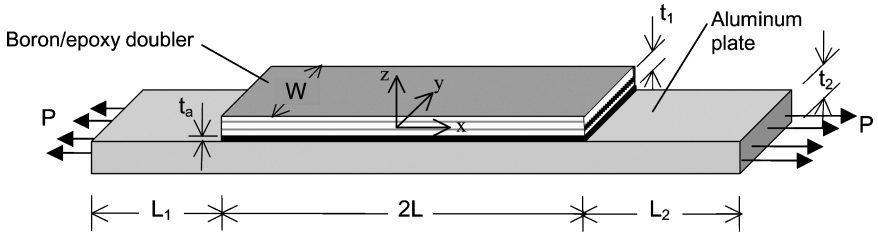

Fig. 2 Configuration of the bonded doubler joint, after Delale et al.[29]

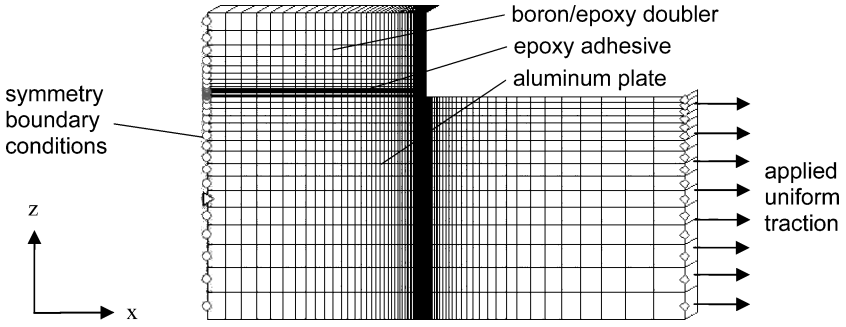

Fig. 3 HOTFGM subcell grid for the bonded doubler joint subjected to uniaxial tension.

(R. L. Actis, personal communication, March 2002), who performed the StressCheck** analyses. The double lap joint configuration is schematically shown in Fig. 5. The doublers and adherends are both composed of T650/F584 graphite/epoxy tape, with $[0_2/90_2]_s$ and $[0_2/90_2]_{2s}$ layups, respectively. The doublers and adherends are bonded using FM300-k adhesive. Figure 6 shows the bilinear constitutive response of the adhesive used in the nonlinear HOTFGM analysis, based on correlation with the experimental adhesive constitutive data given by Tong.[6] The mechanical properties employed for the T650/F581 tape are given in Table 2. In the cases of Mortensen's[19] solution and the HOTFGM linear analysis, the adhesive is treated as linear elastic, whereas nonlinear adhesive properties are used for the remaining cases.

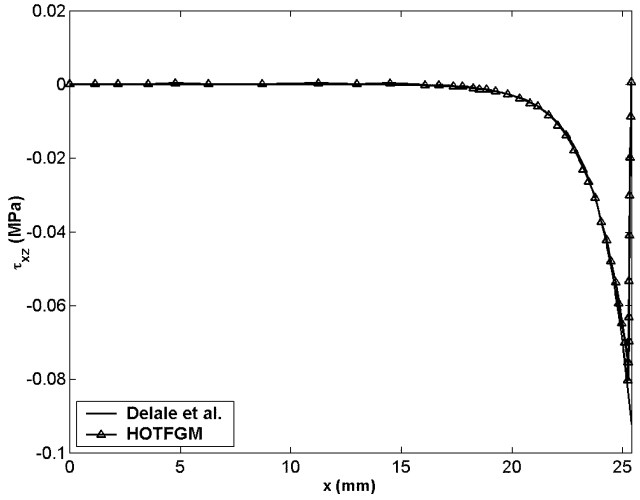

Fig. 4a Adhesive shear stress τ_{xz} in the bonded doubler joint subjected to uniaxial tension as predicted by Delale et al.[29] and HOTFGM.

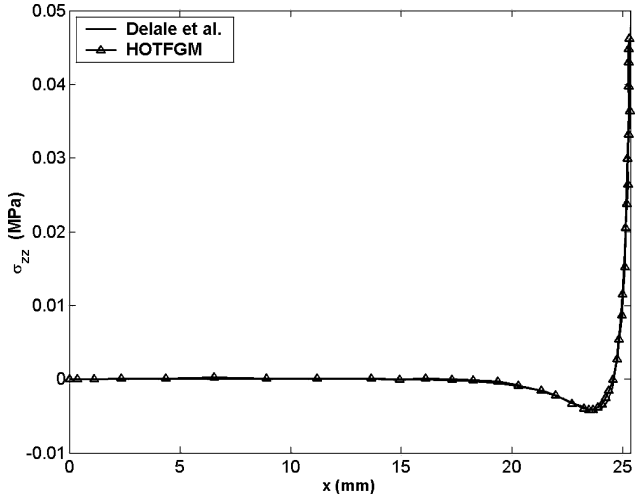

Fig. 4b Adhesive peel stress σ_{zz} in the bonded doubler joint subjected to uniaxial tension as predicted by Delale et al.[29] and HOTFGM.

The analyses of the double lap joint under axial tension were performed using Mortensen's[19] semi-analytical solution and HOTFGM, and the results have been compared with Tong's[6] FEA and experimental results and those of StressCheck. The experimental failure loads reported by Tong[6] range from 1147.0 to 1416.2 kN/m. An average of all reported failure loads (1264.2 kN/m) has been used for comparison. Note that the HOTFGM and Mortensen[19] analyses employed the actual ply lay up for each adherend and doubler laminate. In contrast, the StressCheck (Actis, personal communication) and Tong[6] analyses modeled only the first four plies of each using single layer elements in order to obtain more accurate interlaminar stresses. The remainder of each adherend and doubler was modeled using homogenized laminate properties.

In the HOTFGM analysis, the double lap joint has been discretized into 64 subcells in the x direction and 48 subcells in the z direction (Fig. 7). Forty subcells in the x direction and four subcells in the z direction have been considered in both top and bottom adhesives. Note again that subcell discretization sensitivity studies were used to arrive the employed subcell representation shown in Fig. 7. Symmetric boundary conditions have been applied to the right side of the top and bottom adherends (such that only half of the geometry shown in Fig. 5 is analyzed), and a load of 1264 N/mm or equivalent traction of (1264 N/mm)/(2.23 mm) = 566.8 MPa was applied on the left face of the middle adherend.

Figures 8a and 8b show the adhesive shear and peel stresses predicted by Mortensen's[19] elastic solution and HOTFGM's elastic and nonlinear solutions. Clearly, very good agreement has been achieved

Table 2 Mechanical properties of unidirectional T650/F584 graphite/epoxy tape (nominal ply thickness is 0.14 mm)

Property	Value
Longitudinal modulus E_L	156.5 GPa
Transverse modulus E_T and E_Z	15.65 GPa
Poisson ratio ν_{LT} and ν_{LZ}	0.324
Poisson ratio ν_{TZ}	0.35
Shear modulus G_{LT} and G_{LZ}	5.19 GPa
Shear modulus G_{TZ}	1.53 GPa
Longitudinal tensile strength X_T	2337 MPa
Longitudinal compressive strength X_C	1585 MPa
Transverse tensile strength Y_T and Z_T	46.6 MPa
Interlaminar shear strength R	126.9 MPa

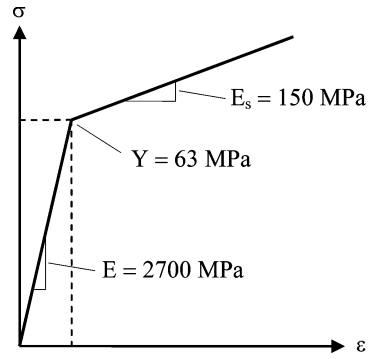

Fig. 6 Bilinear model for FM300-k adhesive used in the HOTFGM nonlinear analysis.

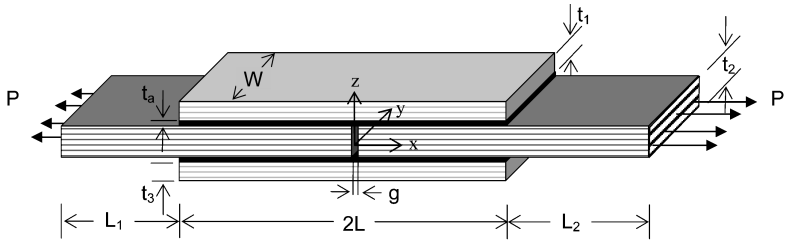

Adherends: T650/F584 tape $[0_2/90_2/]_{2s}$, t_2 = 2.23 mm
Doublers : T650/F584 tape $[0_2/90_2/]_s$, $t_1 = t_3$ = 1.115 mm
Adhesive: FM300-k, t_a = 0.15 mm

Overlap length 2L= 134.2 mm
Outside the overlap $L_1 = L_2$= 30.0 mm
Gap g = 3.04 mm

Fig. 5 Configuration of the bonded double lap joint subjected to uniaxial tension, after Tong.[6]

Table 3 Comparison of adhesive stresses and predicted failure loads

Quantity	HOTFGM linear analysis	HOTFGM nonlinear analysis	Mortensen[19] linear analysis	Tong[6] nonlinear FEM	StressCheck[33] nonlinear FEM[a]	Tong[6] experiment
Max. shear, MPa	93.9	42.2	104.6	~22.0	~32.5	——
Max. peel, MPa	66.7	34.3	73.6	~34.0	~204.0	——
Max. σ_x in the surface ply, MPa	1517.0	1307.0	——	~ 1200	~ 1150.0	——
Predicted failure load, kN/m	707.8[b]	1126.8[b]	654.9[c]	1142.9[b]	1155.8[b]	1264.2

[a]Actis, personal communication. [b]Failure criterion (5). [c]Failure criterion (4).

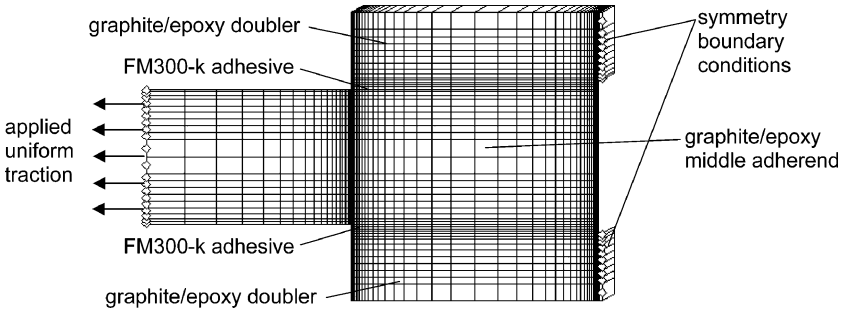

Fig. 7 HOTFGM subcell grid for the double-lap joint.

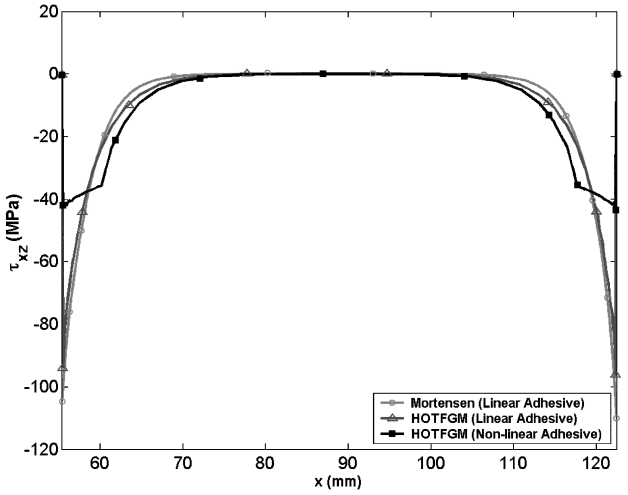

Fig. 8a Adhesive shear stress τ_{xz} in the bonded double lap joint subjected to uniaxial tension.

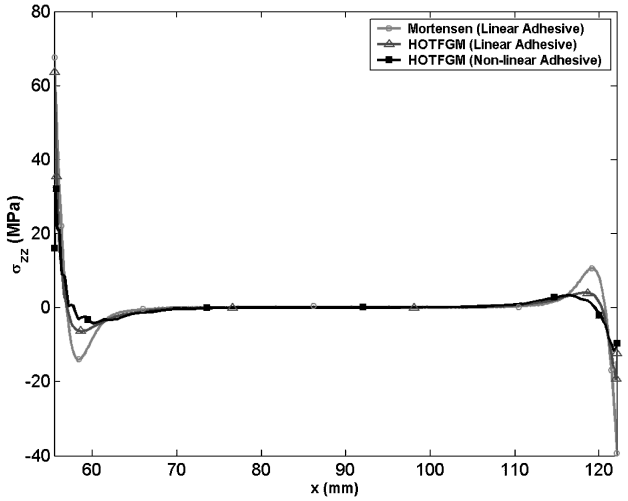

Fig. 8b Adhesive peel stress σ_{zz} in the bonded double lap joint subjected to uniaxial tension.

between the HOTFGM and Mortensen[19] elastic solutions. The effect of yielding in the adhesive is also evident in the HOTFGM results. It can be seen that this nonlinear solution given by HOTFGM predicts much lower peak values of peel and shear stresses at the joint ends. Therefore, plastic deformation of the adhesive will tend to relieve the stress concentration at the leading edges ($x = \pm L$), as also pointed out by Hart-Smith.[18]

Table 3 lists the predicted maximum stress values for the adhesive, the normal stresses in the surface ply of the middle adherend, and the failure loads predicted by each method, as well as the average experimental failure load.[6] Note that the stress values predicted by the Mortensen[19] approach and by HOTFGM were obtained under application of the average failure load $P_a = 1264.2$ kN/m, while the stress values given by Tong[6] and StressCheck (Actis, personal communication) were obtained under application of their reported predicted failure loads. Based on experimental observation, Tong[6] has also suggested interactive failure criteria for bonded adhesive double lap joints containing laminated adherends. These criteria apply to the adherends and are given by

$$\sigma_{zz}^2 / Z^2 + \tau_{xz}^2 / R^2 = 1 \tag{4}$$

which treats the maximum peel and shear stresses as the major contributors to delamination within the surface ply of the adherend, and

$$\frac{\sigma_{xx}^2 - \sigma_{xx}\sigma_{zz}}{X_t X_c} + \frac{\sigma_{zz}^2}{Z^2} + \frac{\tau_{xz}^2}{R^2} = 1 \tag{5}$$

which also accounts for the contribution of normal tensile stress to delamination caused by fiber breakage. Note that the strength parameters appearing in Eqs. (4) and (5) are given in Table 2. By using failure criteria (4) and (5), the failure loads for the linear elastic cases can be predicted by scaling the stress values with respect to the overall loads. The results show that the cases considering the adhesive as linear elastic underestimate the strength of the joint, while the nonlinear analyses generally yield a good estimate of the failure load. Specifically, the HOTFGM and Mortensen[19] linear analyses underpredict the average experimental failure load by 44 and 48%, respectively. The nonlinear analyses still underpredict the failure load, but are within 11% (HOTFGM), 10% (Tong[6]), and 9% [StressCheck (Actis, personal communication)] of the average experimental result. All analyses predict failure by the criterion that includes fiber breakage effects, Eq. (5), except the linear Mortensen[19] analysis, which predicts failure by Eq. (4). Note that the stresses

predicted by the HOTFGM nonlinear analysis given in Table 3 were obtained under the applied axial tension $P = 1264.2$ kN/m, which is not the actual failure load determined by checking with the failure criterion (5). The actual failure load predicted by the HOTFGM nonlinear analysis was obtained through an incremental loading procedure in which the failure criterion (5) is checked at each loading increment. The stress concentration values employed for the Stress-Check failure prediction were not the actual values at the adhesive free edge. Rather, the stress values at a point a certain (undisclosed) distance away from the leading edge were used (Actis, personal communication).

C. Tee Joint

As a final application, HOTFGM was used to analyze so-called "tee joints," the geometries of which are somewhat more complex (Fig. 9) compared to bonded doubler and double lap joints. Apalak et al.[30] analyzed a tee joint with double support, as shown in Fig. 9, using the MSC/NASTRAN finite element package. HOTFGM, like the finite element approach, possesses the geometric versatility required to model the tee joint that is lacking in typical analytical joint analysis methodologies. In addition to the dimensions indicated in Fig. 9 and Table 4, Apalak et al.[30] considered other support lengths a between 10 and 30 mm, which are not considered herein. Further, Apalak et al.[30] explicitly included the adhesive spew fillet in their analyses. This fillet is neglected in the present HOTFGM analyses. The plates as well as the supports were modeled as isotropic steel with the linear elastic properties given in Table 5. Table 5 also provides the isotropic, linear elastic properties for the adhesive material employed by Apalak et al.[30]

Apalak et al.[30] modeled the response of the tee joint to tensile and compressive loading P_1 applied to the top face of the vertical plate as shown in Fig. 10. The present investigation considers only the tensile top face load P_1. Because the loading does not vary along the joint (in the depth direction), the tee-joint problem was treated as plane strain. Two sets of boundary conditions were considered by Apalak et al.,[30] which are also considered herein. The first treats the vertical plate as being bonded to a rigid, or fixed base, and does not actually model the bottom horizontal plate (Fig. 11a). The second set of boundary conditions (Fig. 11b) does include the bottom horizontal plate, with pinned supports on either end at the midpoint of its thickness.

Because of the symmetry of the problem, only one-half of the tee-joint geometry was analyzed using symmetric boundary conditions along the middle of the vertical plate (Fig. 12a). Regarding the magnitude of the applied load, Apalak et al.[30] state that a top face load P_1

Table 4 Tee-joint dimensions (see Fig. 9)

Dimension	Length
Plate length L	100 mm
Plate width (depth) W	100 mm
Support length a	20 mm
Plate/support t Thickness	5 mm
Adhesive thickness δ	0.5 mm

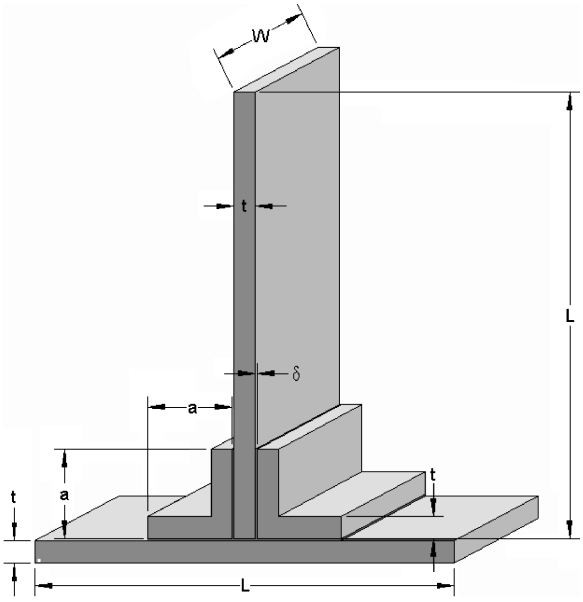

Fig. 9 Tee-joint geometry and dimensions. The steel plates and supports are bonded with a thin adhesive layer.

Table 5 Tee-joint elastic material parameters[30]

Material	Elastic modulus, GPa	Poisson's ratio
Steel	210	0.29
Adhesive	3.33	0.34

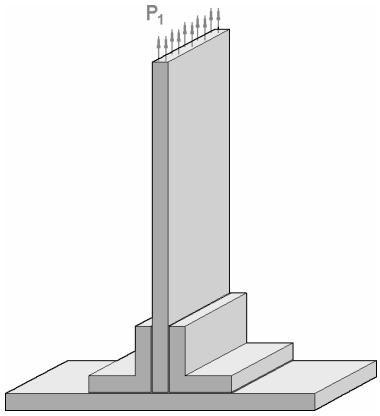

Fig. 10 Top face tensile loading P_1 applied on the tee joint.

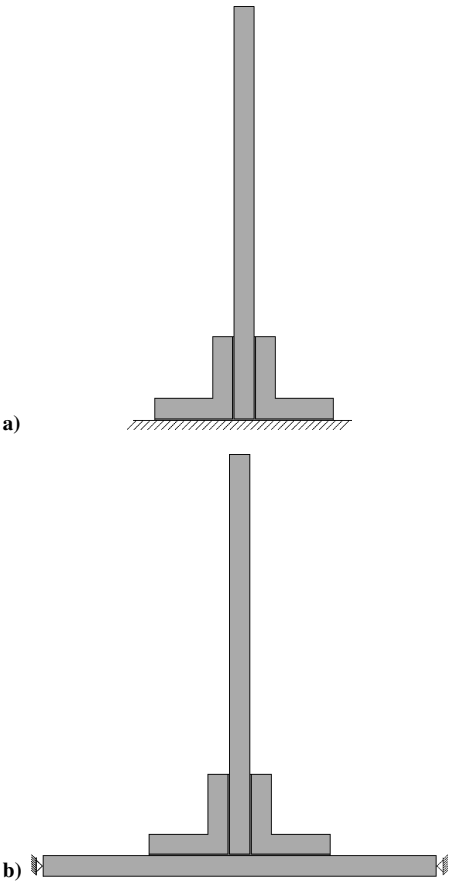

Fig. 11 Tee-joint boundary conditions: a) fixed and b) flexible base.

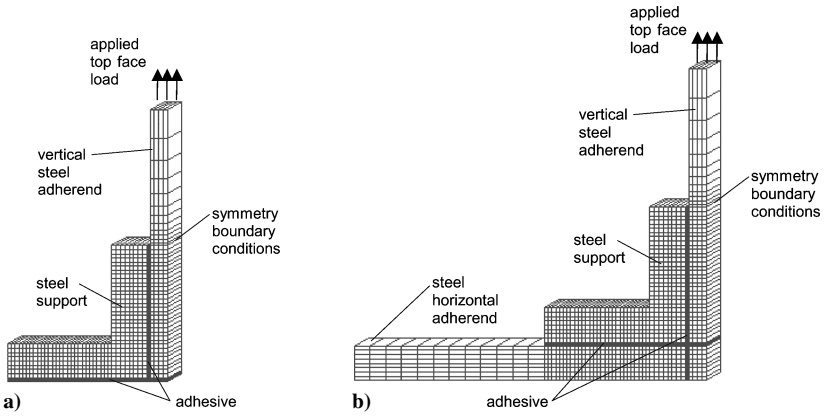

Fig. 12 HOTFGM subcell grid employed for top face tensile loading P_1 for a) fixed- and b) flexible-base boundary conditions.

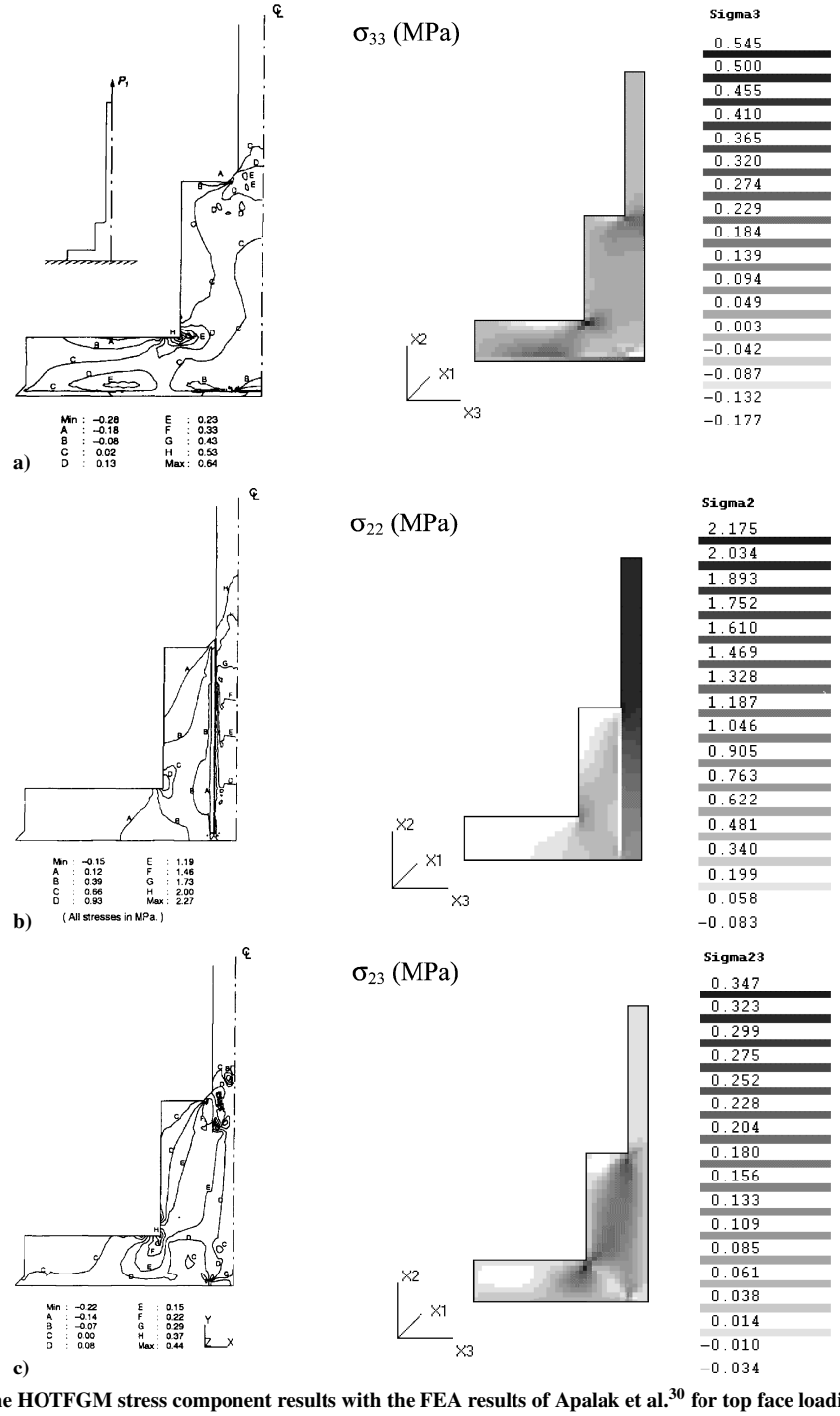

Fig. 13 Comparison of the HOTFGM stress component results with the FEA results of Apalak et al.[30] for top face loading ($P_1 = 5$ N/mm) and fixed support: a) σ_{33}, b) σ_{22}, and c) σ_{23}.

of "500 N mm^{-1}" was applied and distributed "along the upper end of the vertical plate." Conventionally, this statement implies that a load per unit depth of 500 N/mm was distributed along the top face, which has a dimension of $t/2 = 2.5$ mm (because of the employed one-half model with symmetry) (see Fig. 12 and Table 4). Thus the applied tensile traction on the top face in the x_2 direction would be (500 N/mm)/2.5 mm = 200 MPa. However, examining the results presented by Apalak et al.[30] indicates that the tensile normal stress in the vertical plate approaches 2.00 MPa as the distance from the supports increases (Fig. 11b). Thus, it is most likely that Apalak et al.[30] actually employed a total load of $P_1 = 500$ N, which was distributed over the entire one-half model top face of dimensions $W \times \frac{1}{2}t$ such that $\sigma_{22} = (500\text{ N})/(100\text{ mm} \times 2.5\text{ mm}) = 2.00$ MPa. Therefore, the load per unit depth P_1 employed herein is 500 N/100 mm = 5 N/mm. For additional details, see Bednarcyk and Yarrington.[32]

Figure 12 shows the HOTFGM subcell grids employed for the two sets of boundary conditions. Recall that, because of the use of symmetry conditions along the right boundary in Fig. 12, only one-half of the tee-joint geometry is modeled (see Fig. 10). In addition, in association with subcell discretization sensitivity studies, it was determined that employing the full 100-mm length of the vertical plate was not necessary. Provided the top face of the vertical plate (where the load is applied) is sufficiently far from the joint, the HOTFGM results are identical for much smaller vertical plate lengths. To reduce the number of subcells required, a vertical plate length of 40 mm was employed (Fig. 12).

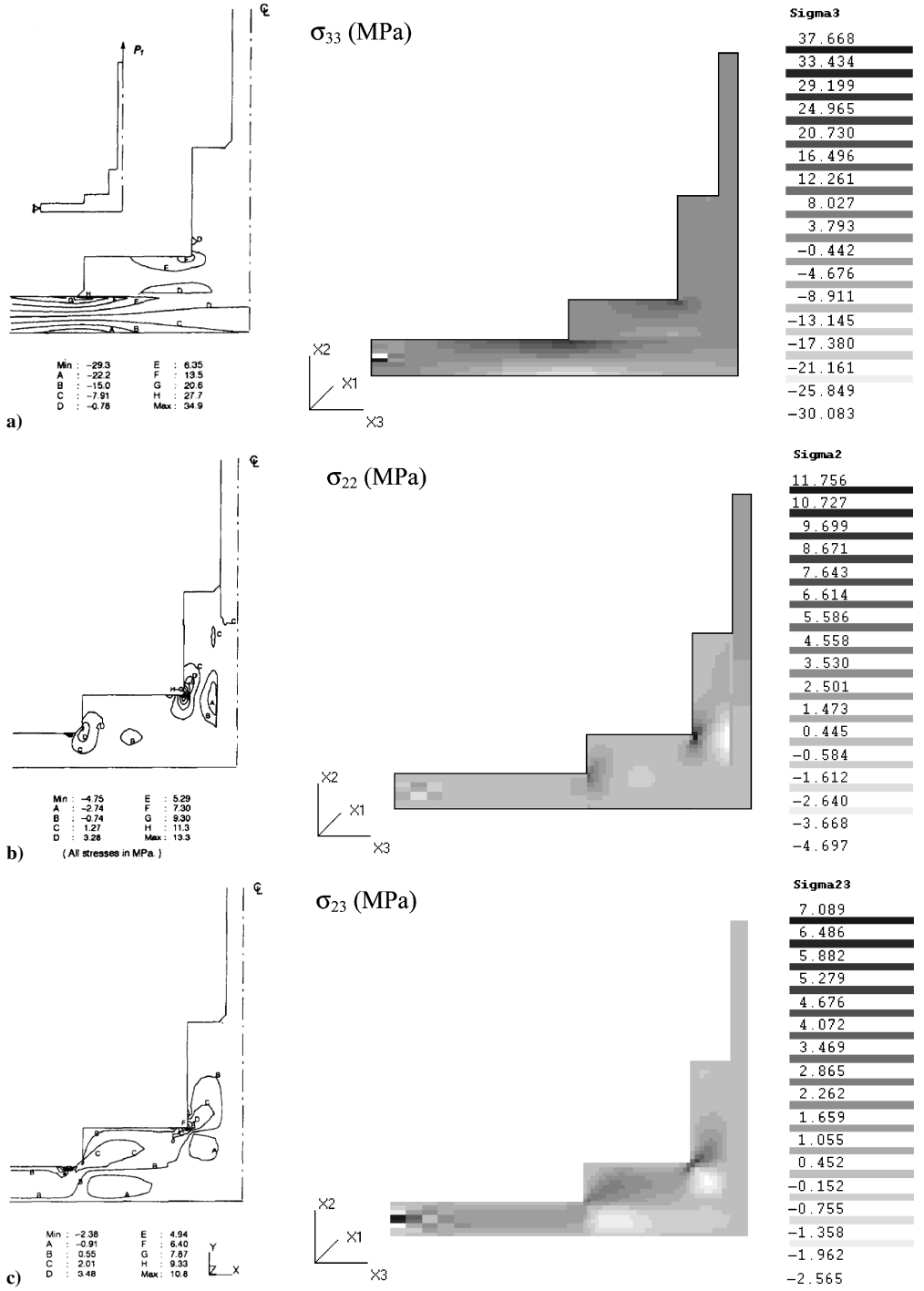

Fig. 14 Comparison of the HOTFGM stress component results with the FEA results of Apalak et al.[30] for top face loading ($P_1 = 5$ N/mm) and flexible support: a) σ_{33}, b) σ_{22}, and c) σ_{23}.

Table 6 Comparison of stress component concentrations for the tee joint as predicted by HOTFGM and Apalak et al.[30]

	Concentration, MPa			
	Fixed support		Flexible support	
Stress	Apalak et al.[30]	HOTFGM	Apalak et al.[30]	HOTFGM
Max. σ_{33}	0.64	0.55	34.9	37.67
Min. σ_{33}	−0.28	−0.18	−29.3	−30.08
Max. σ_{22}	2.27	2.18	13.3	11.76
Min. σ_{22}	−0.15	−0.083	−4.75	−4.70
Max. σ_{23}	0.44	0.35	10.8	7.09
Min. σ_{23}	−0.22	−0.03	−2.38	−2.57

Both the horizontal and vertical plates, as well as the supports, were modeled using eight through-thickness subcells. The adhesive, though much thinner, was also modeled using eight through-thickness subcells. The fixed-base boundary condition grid employed a total of 1296 subcells, while the flexible base grid employed a total of 1776 subcells. In the case of the flexible base, the pinned boundary condition (see Fig. 11b) was imposed by fixing (i.e., imposing zero average displacement to) the middle two subcells of the horizontal plate along the left face.

Figures 13 and 14 compare the HOTFGM predicted stress fields with the FEA results of Apalak et al.[30] for the two sets of boundary conditions (see Fig. 11). The FEA results show only a part of the analyzed geometry, whereas the HOTFGM results show the entire geometry analyzed. Despite the fact that the HOTFGM analyses did not explicitly model the adhesive spew fillet as was done in the FEA models, the agreement between HOTFGM and FEA is excellent. Qualitatively, the stress fields are virtually identical. Quantitatively, although the absolute minimum and maximum values quoted in the FEA results differ slightly from those evident in the HOTFGM results (see Table 6), comparing the actual contours between the two sets of results indicates excellent agreement. Further, some discrepancy in the highest concentrations predicted is expected because of the highly refined mesh employed by Apalak et al.[30] in joint and fillet regions. Finally, the HOTFGM results in Fig. 14, which show the entire half model of the bottom plate, indicate stress concentrations associated with the boundary condition applied along the left face of the horizontal plate. Because Apalak et al.[30] showed only a detail of the geometry in their results, it is unclear whether or not a similar concentration is present in the FEA results.

It is clear that HOTFGM does a good job of analyzing the tee-joint problem for both fixed and flexible support conditions. In addition, HOTFGM is very efficient, not only in terms of the model execution time, but also in terms of the analysis cycle time required to set up the problem and postprocess the results. The actual execution time was approximately 6.5 s for the fixed-base problem and 6.9 s for the flexible-base problem, where a 2.5-GHz desktop computer with 1 GB of RAM was used.

IV. Conclusions

A new application of the higher-order theory for functionally graded materials (HOTFGM) to the adhesively bonded joint problem was presented in this paper. Like the finite element method, HOTFGM considers a discretized geometry, but exhibits considerably less mesh dependence as the continuity and field equations (heat transfer and equilibrium) are satisfied in a surface- and volume-averaged sense, respectively. The present investigation employs HOTFGM to analyze adhesively bonded doubler, double lap, and tee joints. Results have been compared to the recently developed solutions of Mortensen[19] for the double lap joint and the closed-form solution of Delale et al.[29] for the bonded doubler joint. In addition, the HOTFGM and Mortensen[19] double lap joint results have been compared the h-based FEA results of Tong[6] and p-based FEA results from StressCheck.** Good agreement has been achieved between HOTFGM and Mortensen's[19] elastic solution. Finally, HOTFGM was employed to analyze a more complex joint geometry (a so-called tee joint) for which analytical models are lacking, and results were compared to the h-based FEA results of Apalak et al.[30] The results of this paper indicate that HOTFGM is useful and accurate for the analysis of adhesively bonded joints, even in terms of inelastic analysis and failure load prediction. The approach appears to embody a middle ground spanning the accurate and versatile yet cumbersome finite element approach and the efficient yet less general analytical approach.

References

[1]HyperSizer Structural Sizing Software, Collier Research Corp., Hampton, VA, 1998.

[2]Kairouz, K. C., and Matthews, F. L., "Strength and Failure Modes of Bonded Single Lap Joints Between Cross-Ply Adherends," *Composites*, Vol. 24, No. 6, 1993, pp. 475–484.

[3]Shenoi, R. A., and Hawkins, G. L., "An Investigation into the Performance of Top-Hat Stiffener to Shell Plating Joints," *Composite Structures*, Vol. 30, No. 1, 1995, pp. 109–121.

[4]Tsai, M. Y., Morton, J., and Matthews, F. L., "Experimental and Numerical Studies of a Laminated Composite Adhesive Joint," *Journal of Composite Materials*, Vol. 29, No. 9, 1995, pp. 1254–1275.

[5]Yamazaki, K., and Tsubosaka, N., "A Stress Analysis Technique for Plate and Shell Built-Up Structures with Junctions and Its Application to Minimum-Weight Design of Stiffened Structures," *Structural Optimization*, Vol. 14, No. 2–3, 1997, pp. 173–183.

[6]Tong, L., "An Assessment of Failure Criteria to Predict the Strength of Adhesively Bonded Composite Double Lap Joints," *Journal of Reinforced Plastics and Composites*, Vol. 6, No. 18, 1997, pp. 699–713.

[7]Li, G., Lee-Sullivan, P., and Thring, R. W., "Nonlinear Finite Element Analysis of Stress and Strain Distributions Across the Adhesive Thickness in Composite Single-Lap Joints," *Composite Structures*, Vol. 46, No. 4, 1999, pp. 395–403.

[8]Krueger, R., Cvitkovich, M. K., O'Brien, T. K., and Minguet, P. J., "Testing and Analysis of Composite Skin/Stringer Debonding Under Multi-Axial Loading," NASA TM-1999-209097, Feb. 1999.

[9]Krueger, R., Minguet, P. J., and O'Brien, T. K., "A Method for Calculating Strain Energy Release Rates in Preliminary Design of Composite Skin/Stringer Debonding Under Multi-Axial Loading," NASA TM-1999-209365, July 1999.

[10]Bogdanovich, A. E., and Kizhakkethara, I., "Three-Dimensional Finite Element Analysis of Double-Lap Composite Adhesive Bonded Joints Using Submodeling Approach," *Composites: Part B*, Vol. 30, No. 6, 1999, pp. 537–551.

[11]Volkersen, O., "Die Nietkraftoerteilung in Ubeansprunchten Nietverbindungen mit Konstanten Loshonquerschnitten," *Luftfahrtforschung*, Vol. 15, No. 1/2, 1938, pp. 41–47.

[12]Goland, M., and Reissner, E., "The Stresses in Cemented Joints," *Journal of Applied Mechanics*, Vol. 11, No. 1, 1944, pp. A17–A27.

[13]Hart-Smith, L. J., "Adhesive-Bonded Double-Lap Joints," NASA CR-112235, Jan. 1973.

[14]Hart-Smith, L. J., "Adhesive-Bonded Single-Lap Joints," NASA CR-112236, Jan. 1973.

[15]Hart-Smith, L. J., "Adhesive-Bonded Scarf and Stepped-Lap Joints," NASA CR-112237, Jan. 1973.

[16]Hart-Smith, L. J., "Adhesive Bond Stresses and Strains at Discontinuities and Cracks in Bonded Structures," *Journal of Engineering Materials and Technology*, Vol. 100, No. 1, 1978, pp. 16–24.

[17]Hart-Smith, L. J., "Differences Between Adhesive Behavior in Test Coupons and Structural Joints," Douglas Aircraft Co., Paper 7066, Long Beach, CA, March 1981.

[18]Hart-Smith, L. J., "Design Methodology for Bonded-Bolted Composite Joints," Douglas Aircraft Co., U.S. Air Force CR AFWAL-TR-81-3154, Vols. 1 and 2, Wright–Patterson AFB, OH, Feb. 1982.

[19]Mortensen, F., "Development of Tools for Engineering Analysis and Design of High-Performance FRP-Composite Structural Elements," Ph.D. Dissertation, Inst. of Mechanical Engineering, Aalborg Univ., Special Rept. 37, Aalborg, Denmark, Aug. 1998.

[20]Mortensen, F., and Thomsen, O. T., "Analysis of Adhesive Bonded Joints: A Unified Approach," *Composites Science and Technology*, Vol. 62, No. 7–8, 2002, pp. 1011–1031.

[21]Mortensen, F., and Thomsen, O. T., "Coupling Effects in Adhesive Bonded Joints," *Composite Structures*, Vol. 56, No. 2, 2002, pp. 165–174.

[22]Aboudi, J., Pindera, M.-J., and Arnold, S. M., "Higher-Order Theory for Functionally Graded Materials," *Composites: Part B*, Vol. 30, No. 8, 1999, pp. 777–832.

[23]Aboudi, J., Pindera, M.-J., and Arnold, S. M., "Thermoelastic Response of Large-Diameter Fiber Metal Matrix Composites to Thermal Gradients," NASA TM-106344, Oct. 1993.

[24]Aboudi, J., Pindera, M.-J., and Arnold, S. M., "Microstructural Optimization of Functionally Graded Composites Subjected to a Thermal Gradient Via the Coupled Higher-Order Theory," *Composites: Part B*, Vol. 28, No. 1–2, 1997, pp. 93–108.

[25]Pindera, M.-J., Aboudi, J., and Arnold, S. M., "Limitations of the Uncoupled, RVE-Based Micromechanical Approach in the Analysis of Functionally Graded Composites," *Mechanics of Materials*, Vol. 20, No. 1, 1995, pp. 77–94.

[26]Pindera, M.-J., and Dunn, P., "Evaluation of the Higher-Order Theory for Functionally Graded Materials via the Finite Element Method," *Composites: Part B*, Vol. 28, No. 1–2, 1997, pp. 109–119.

[27]Arnold, S. M., Bednarcyk, B. A., and Aboudi, J., "Analysis of Internally Cooled Structures Using a Higher Order Theory," *Computers and Structures*, Vol. 82, No. 7–8, 2004, pp. 659–688.

[28]Bansal, Y., and Pindera, M.-J., "Efficient Reformulation of the Thermoelastic Higher-Order Theory for Functionally Graded Materials," *Journal of Thermal Stresses*, Vol. 26, No. 11–12, 2003, pp. 1055–1092.

[29]Delale, F., Erdogan, F., and Aydinoglu, M. N., "Stresses in Adhesively Bonded Joints: A Closed-Form Solution," *Journal of Composite Materials*, Vol. 15, May 1981, pp. 249–271.

[30]Apalak, Z. G., Apalak, M. K., and Davies, R., "Analysis and Design of Tee Joints with Double Support," *International Journal of Adhesion and Adhesives*, Vol. 16, No. 3, 1996, pp. 187–214.

[31]Mendelson, A., *Plasticity: Theory and Application*, Krieger, Malabar, FL, 1968.

[32]Bednarcyk, B. A., and Yarrington, P. W., "Elasto-Plastic Analysis of Tee Joints Using HOT-SMAC," NASA CR-2004-213067, May 2004.

B. Sankar
Associate Editor